

Atmospheric effects

- Background
- Extinction
- Differential refraction
- Seeing

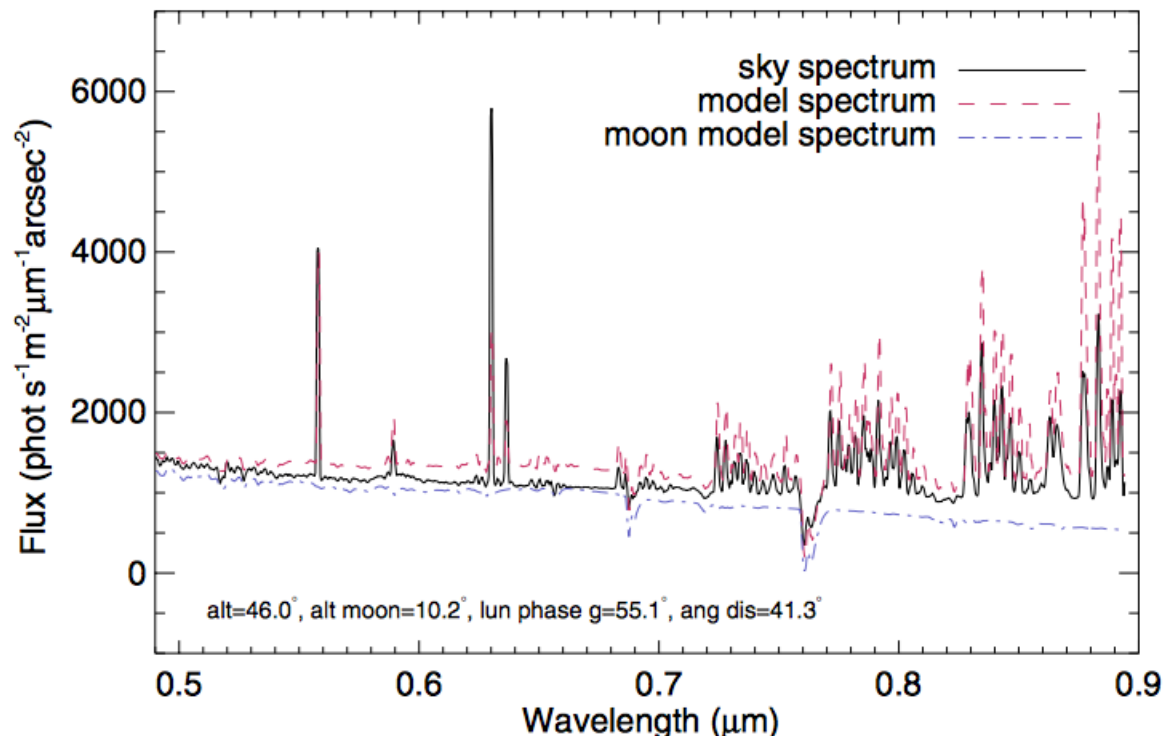
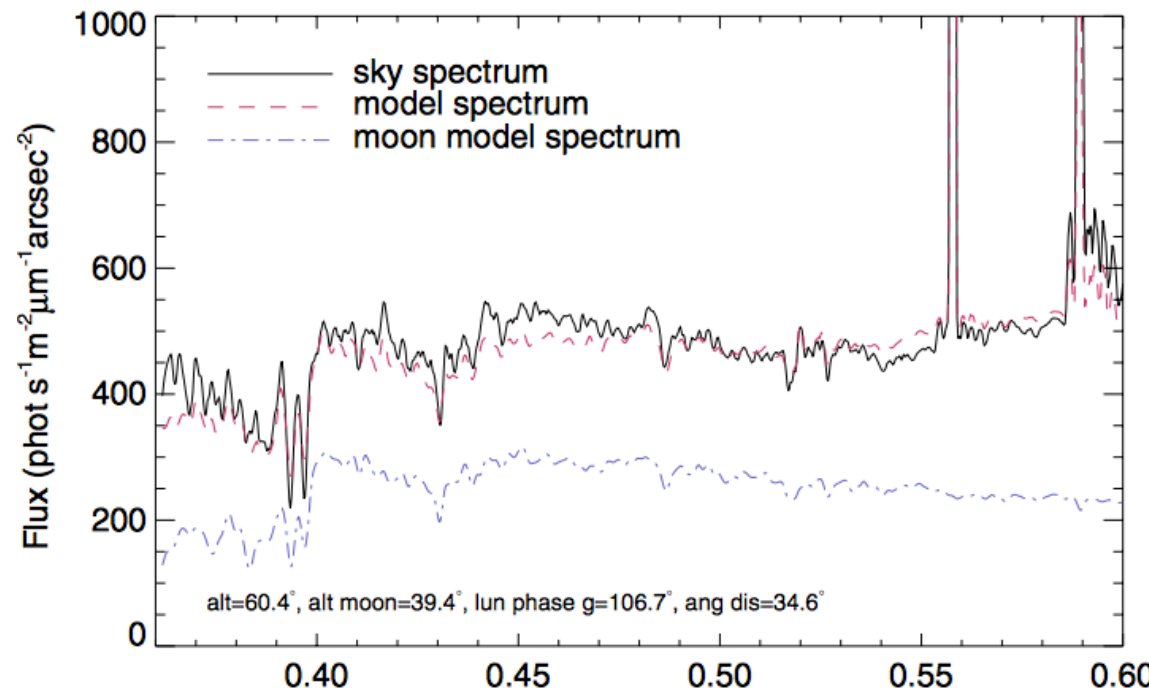
Atmospheric Background

Calculated sky brightness model compared with observations from FORS 1 at Paranal (A Jones et al 2013)

The two plots compare models with different contributions from scattered moonlight, which is the dominant source of background under bright sky conditions

The strong narrow features are OI] and NI airglow lines, which are variable, so intensities will not match a general model. OH emission becomes prominent longwards of 700nm

Note that the scattered light background is quite strongly polarized



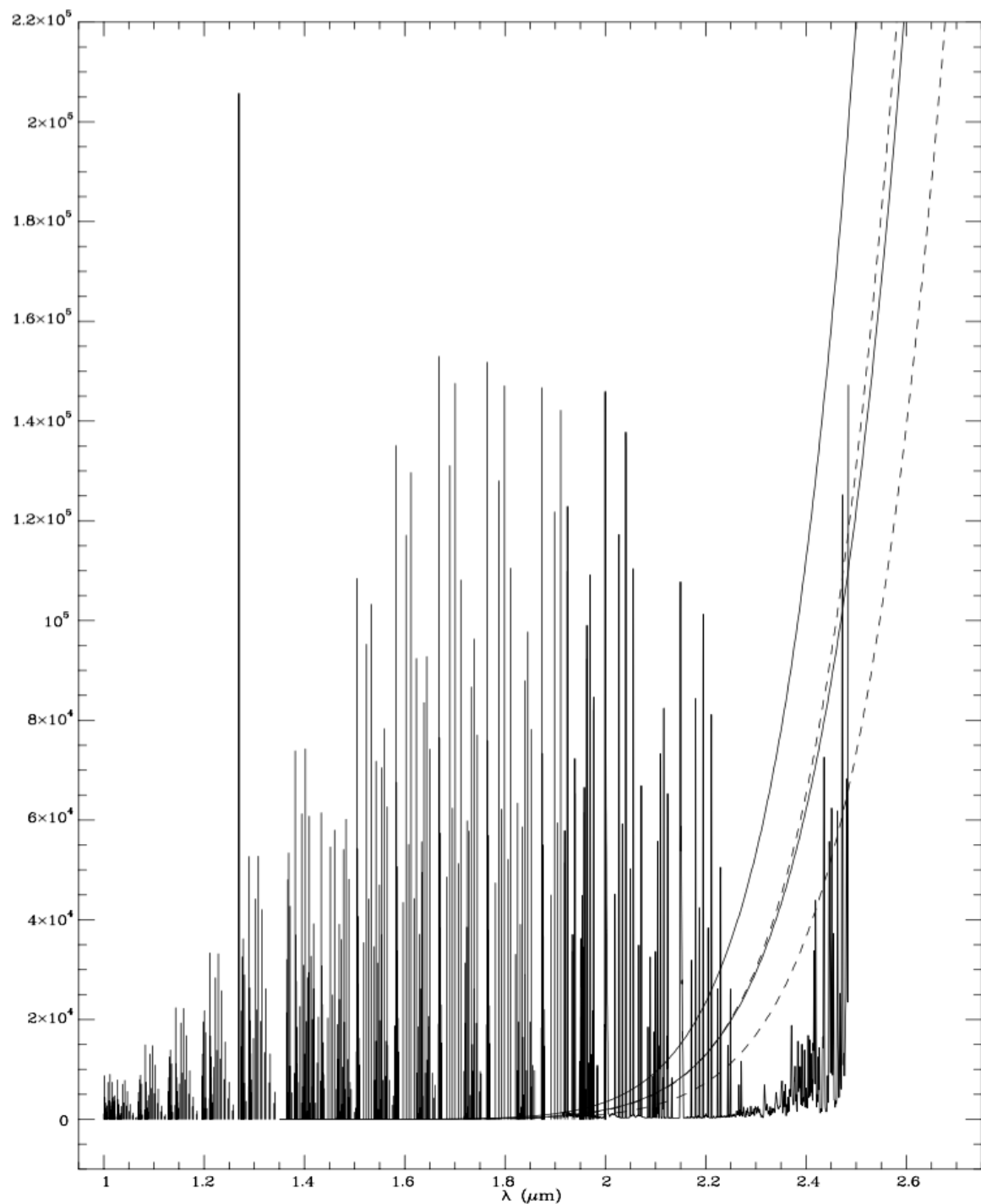
Near Infrared Sky Emission

Airglow lines from OH + O₂ emit strongly at far-red and near-IR wavelengths.

They are temporally and spatially variable and reduce sensitivity markedly.

Sites away from the geomagnetic poles are preferred

Model sky spectrum including airglow lines, thermal emission from the atmosphere with thermal emission from the telescope indicated by the continuous and dashed lines in summer and winter for high and low emissivities



Mid- Infrared Emission

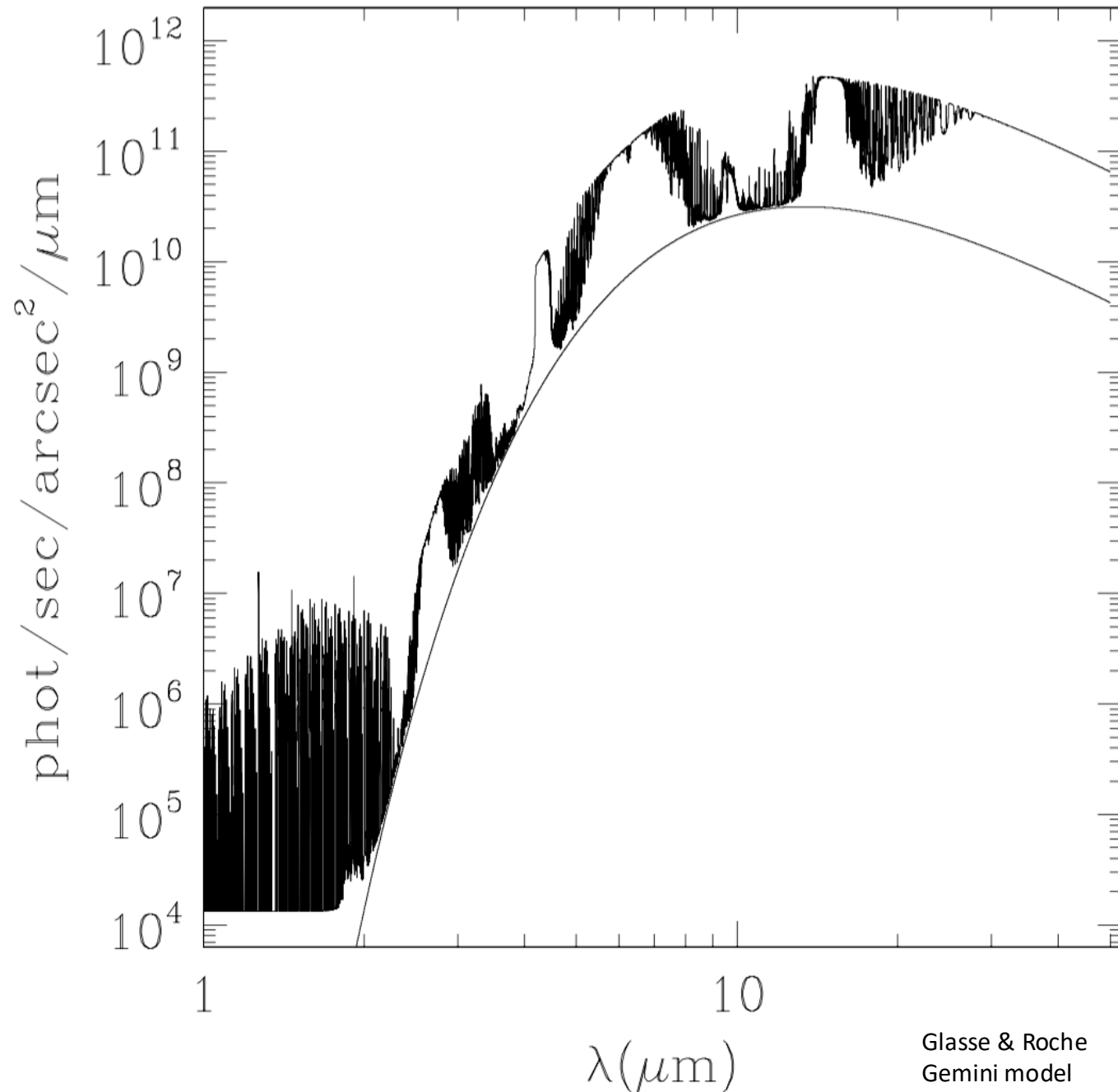
At mid-infrared wavelengths, the thermal emission from the sky dominates

It peaks at $\sim 12\mu\text{m}$ and leads to an enormous photon flux

Careful control of telescope emissivity and cold, dry sites are preferred.

In this model a telescope and sky temperature of 275K (winter on MK) is used with a system emissivity of 7%

MK 1.2mm PWV 275 K $e=7\%$



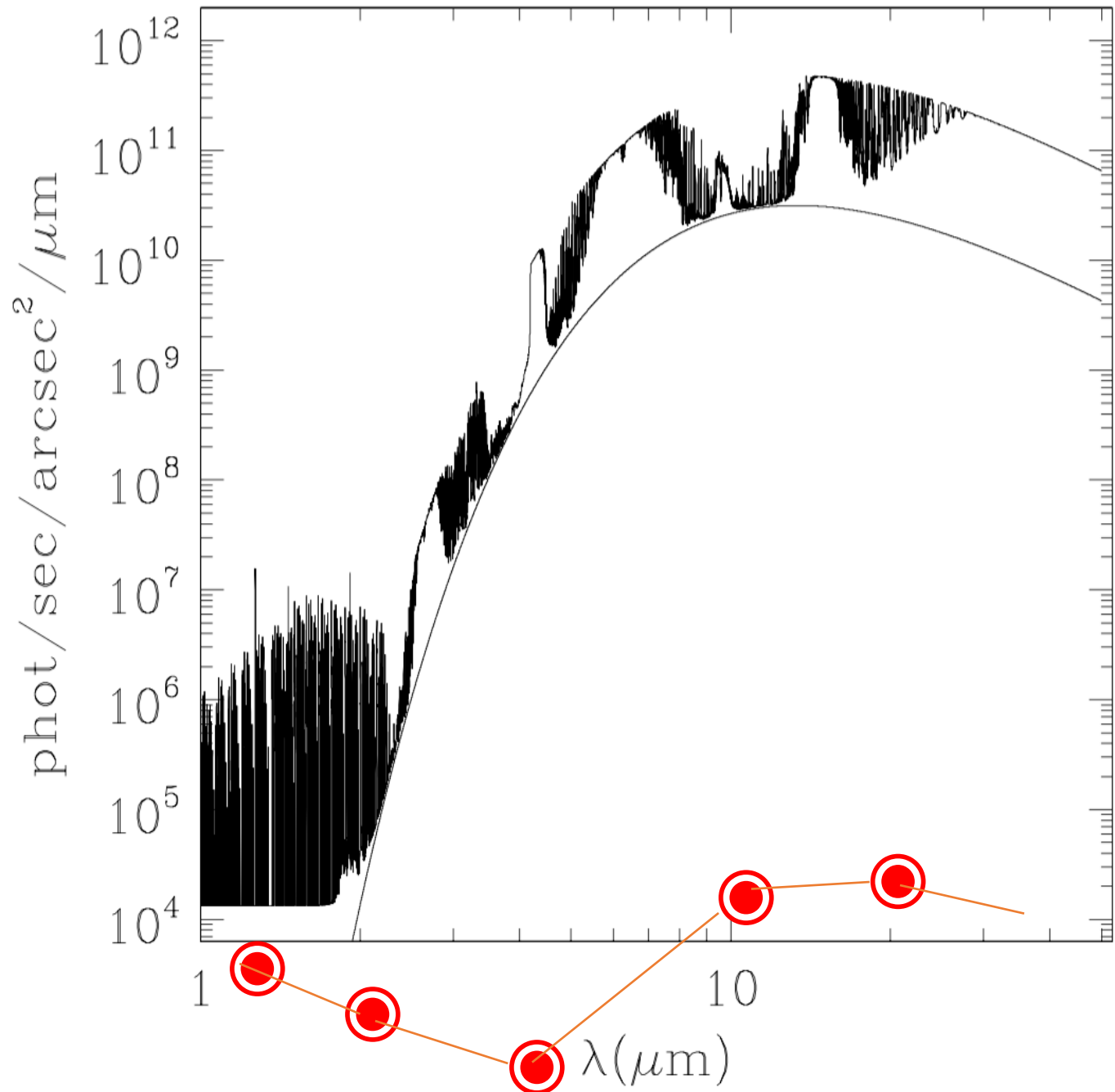
Mid- Infrared in Space

JWST is a passively cooled telescope at L2, launched in 2021

It is optimised for IR observations, taking advantage of the low sky background, and should be limited by zodiacal light from the solar system at $\lambda < 10\mu\text{m}$

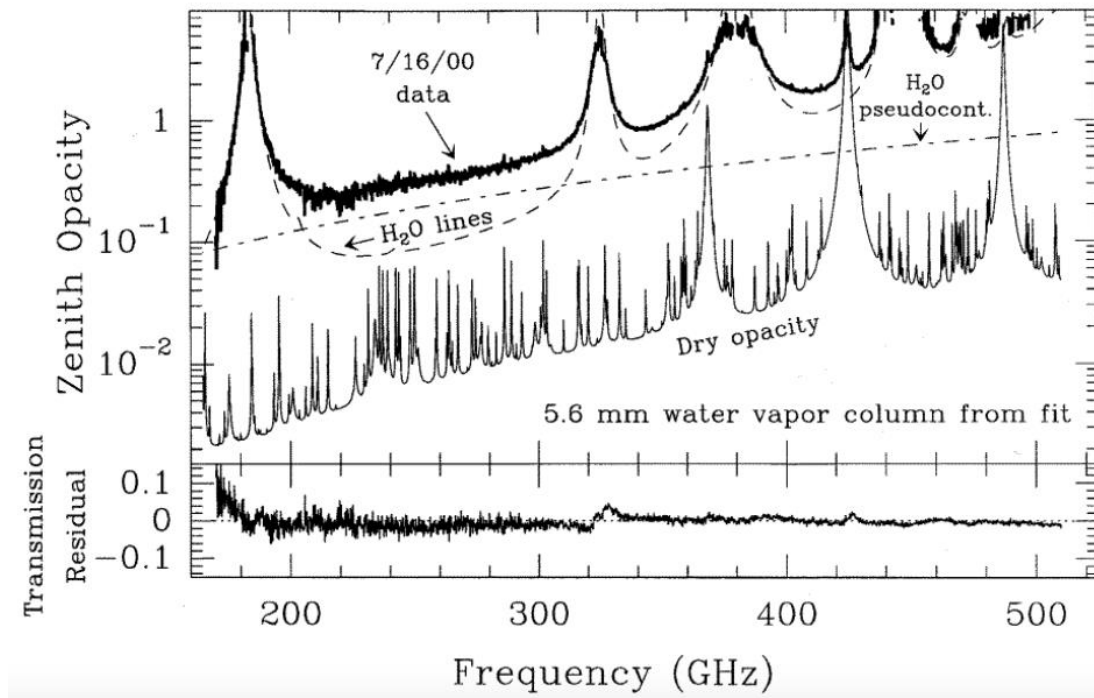
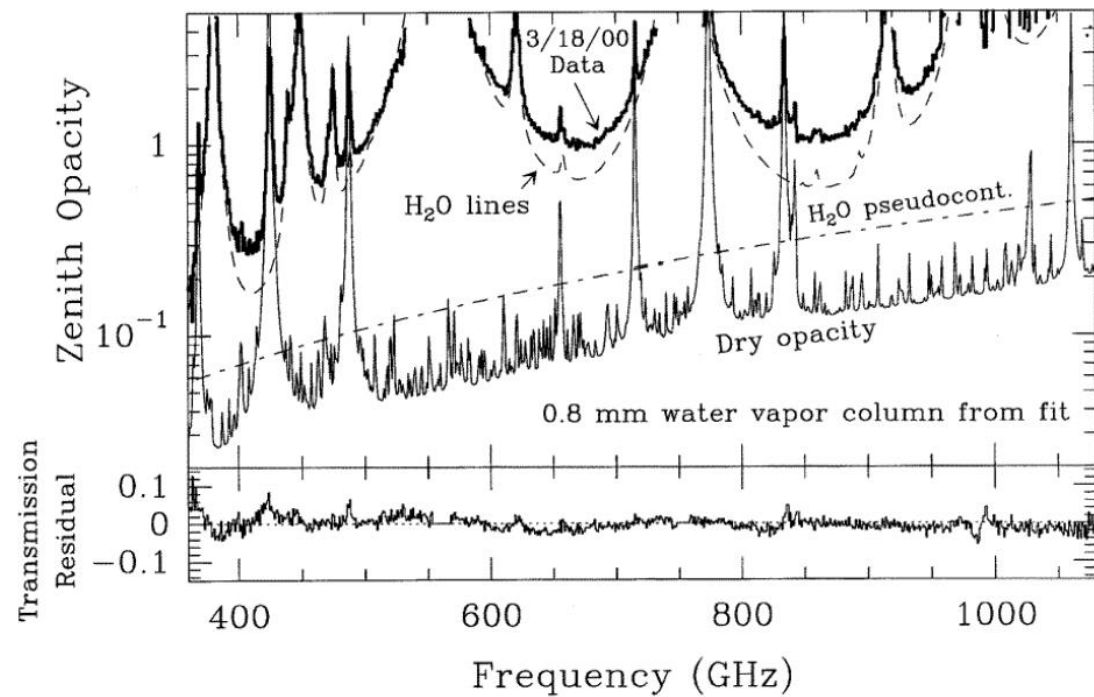
The photon background from the ZL at L2 is indicated by 

MK 1.2mm PWV 275 K e=7%



Sub-mm Sky Emission at MK

- FTS zenith atmospheric opacity spectra obtained on Mauna Kea in March and July 2000 and best fit opacity contributions
- The fitting routine that produced these results is based on the radiative transfer code and uses only the precipitable water vapor column as a free parameter
(J R Pardo et al 2001)



Artificial Backgrounds

- City Lights,
- Dust
- Radio Frequency Interference
 - Broadcasts, mobile phones, microwaves, other equipment on site
- Satellites – reflected sunlight & comms
- Aircraft con trails etc
- Laser light from LGS
- + cosmic rays

- Plus Volcanic aerosols, Saharan dust etc

Optical/NIR Sky brightness values

Filter	Continuum brightness	
	[$\gamma/s/\mu m/m^2/arcsec^2$]	[mag/arcsec ²]
U	190	21.5
B	150	22.4
V	210	21.7
Rc	340	20.8
Ic	500	19.9
J	1200	18.0
H	2300	16.5
K	2300	15.7

Sky Brightness (mag/arcsec ²)					
lunar age (days)	U	B	V	R	I
0	22.0	22.7	21.8	20.9	19.9
3	21.5	22.4	21.7	20.8	19.9
7	19.9	21.6	21.4	20.6	19.7
10	18.5	20.7	20.7	20.3	19.5
14	17.0	19.5	20.0	19.9	19.2

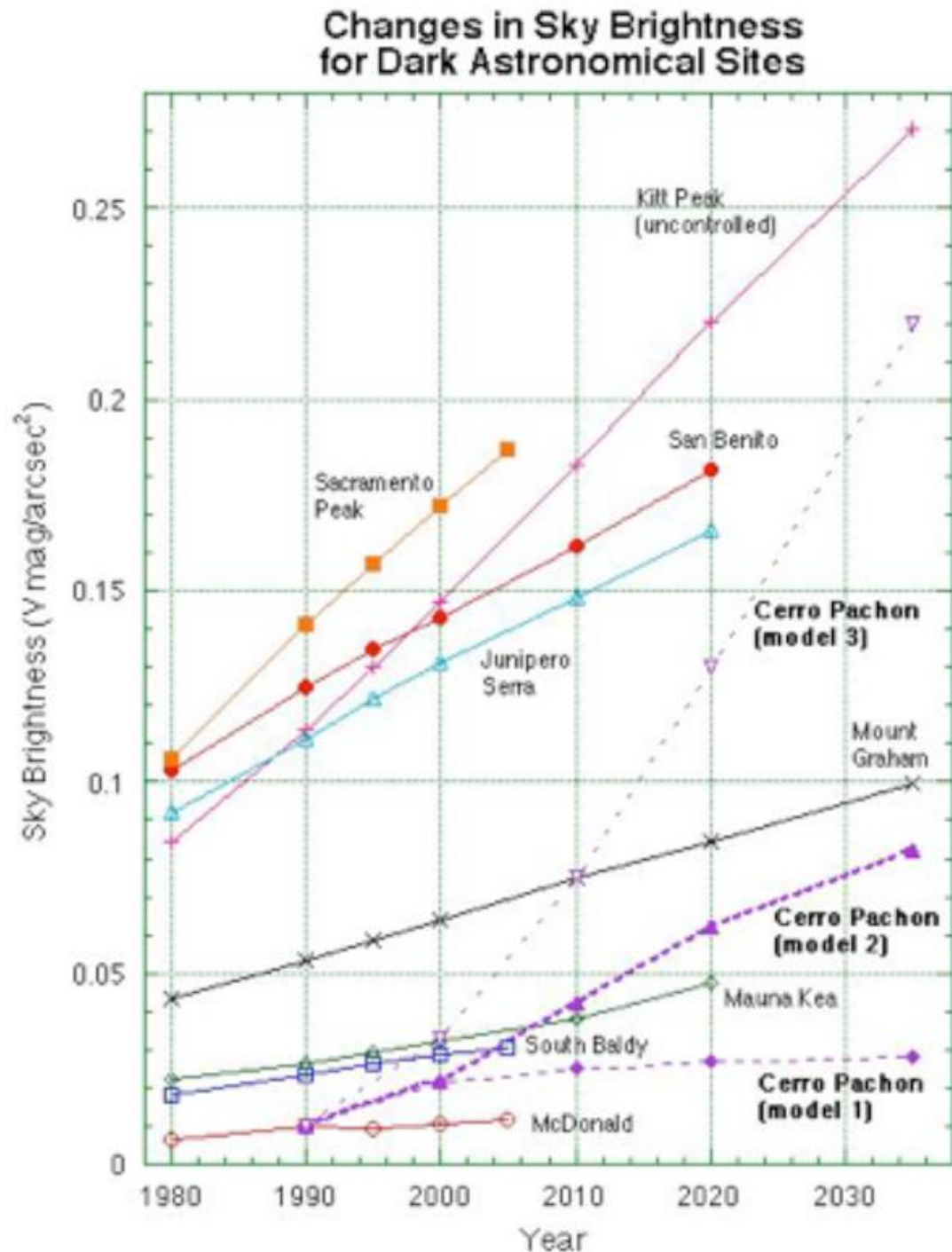
Paranal Sky Brightness at 3 days and variation with lunar phase

Dark Sky Protection

Threats from increasing populations, urban sprawl and Industrial developments

Education and Implementation and enforcement of Lighting Ordinances

Installation of light shields
Low pressure sodium lighting



Atmospheric Extinction under good conditions (Mauna Kea CFHT)

wavelength	mag/airmass	wavelength	mag/airmass
(nm)			
• 300	4.90	425	0.21
• 310	1.37	450	0.17
• 320	0.82	475	0.14
• 330	0.57	500	0.13
• 340	0.51	525	0.12
• 350	0.42	550	0.12
• 360	0.37	575	0.12
• 370	0.33	600	0.11
• 380	0.30	650	0.11
• 390	0.27	700	0.10
• 400	0.25	800	0.07
		900	0.05

IR Atmospheric Extinction under good conditions (Mauna Kea UKIRT)

Wavel/Filter	mean (mag/air mass)	median (mag/air mass)
(0.36) U	0.358	0.358
(0.44) B	0.198 +/- 0.008	0.194
(0.55) V	0.119 0.005	0.111
(1.25) J	0.114 0.007	0.102
(1.65) H	0.068 0.006	0.059
(2.2) K	0.096 0.005	0.088
(3.4) L	0.203 0.030	0.150
(3.8) L'	0.112 0.009	0.093
(4.8) M	0.244 0.016	0.220
(10) N	0.184 0.017	0.151
(20) Q	0.503 0.030	0.451

Extinction Variations

- Mean or median extinction values are a useful guide, but the values to be used on a given night generally have to be calculated for the night.
- Thin cloud, dust etc can have a marked effect even on a usable night.

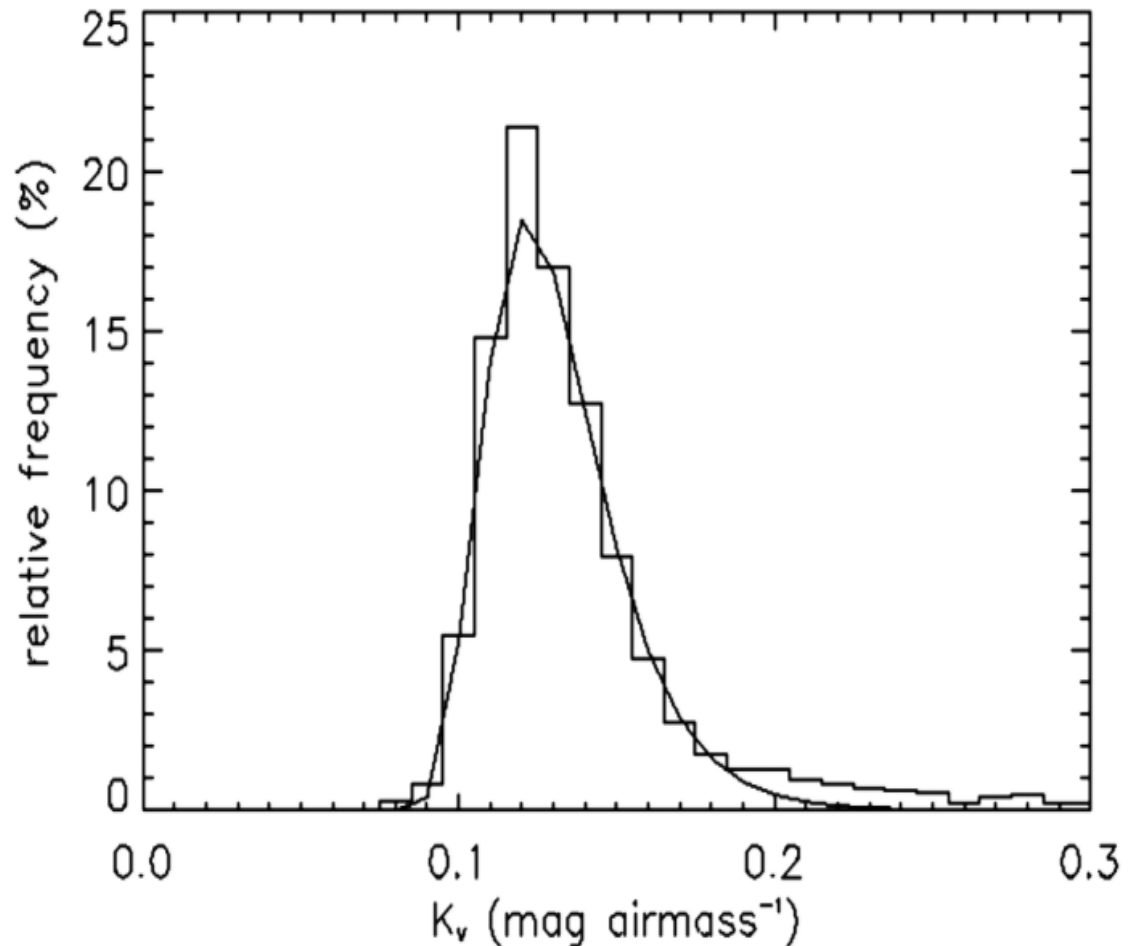
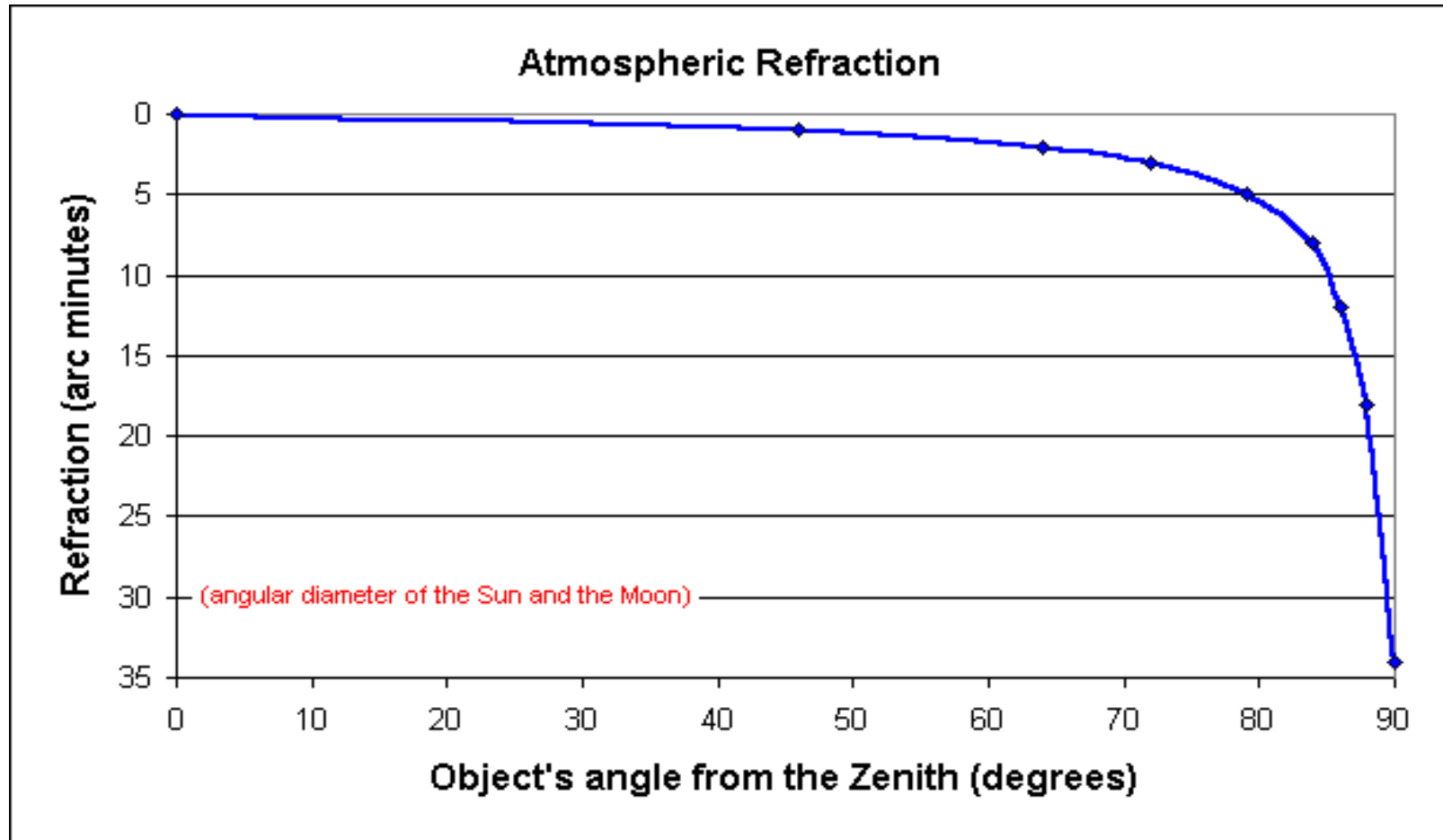


FIG. 7.—Histogram of the relative frequency of k_V for nonsummer nights V Band opacity for LaPalma over 20yr (A Garcia-Gil 2010)

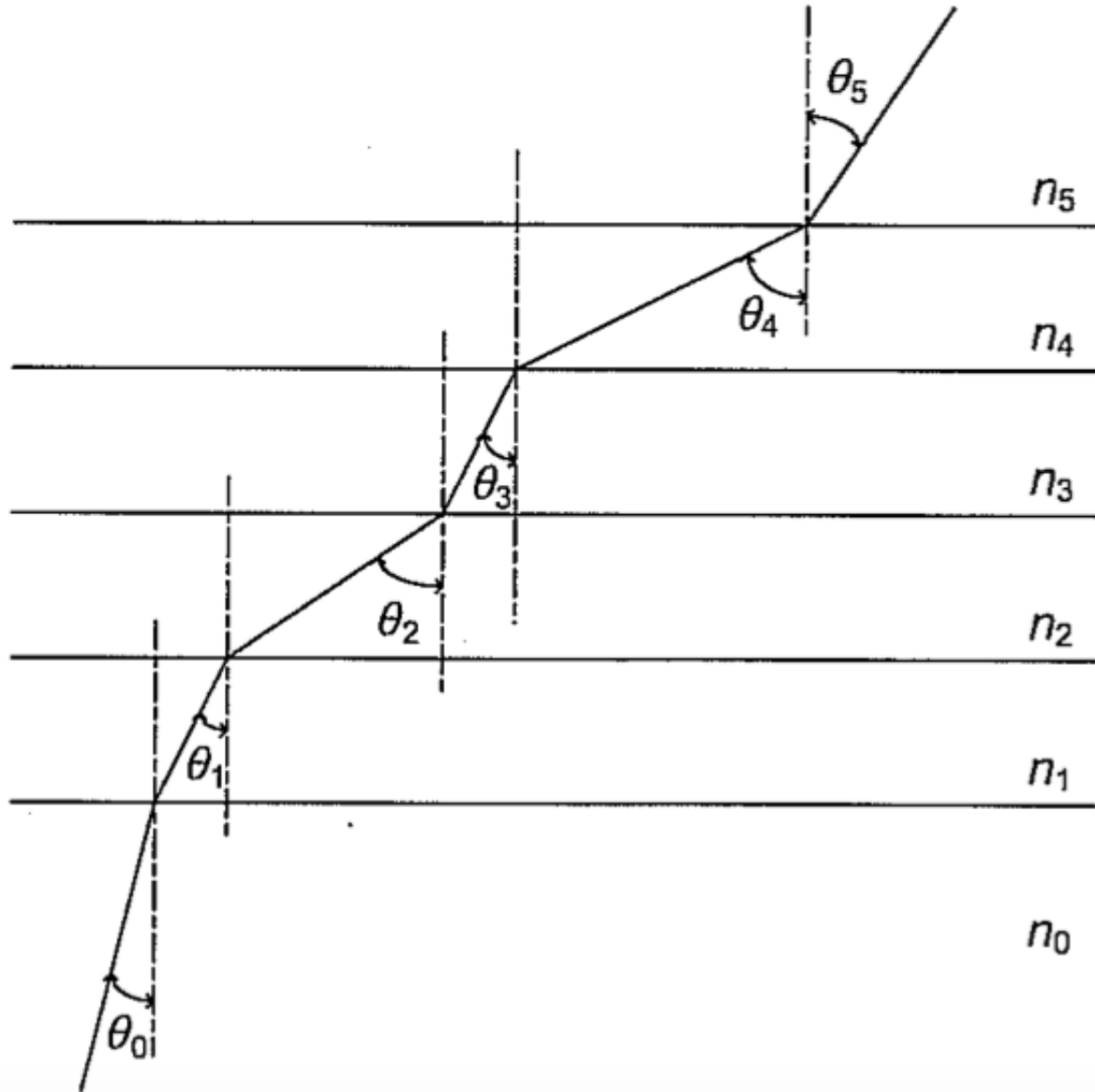
Atmospheric Refraction



- Observations made away from the zenith pass through atmospheric layers at an angle, leading to increasing refraction with zenith distance.

Refraction at different atmospheric layers

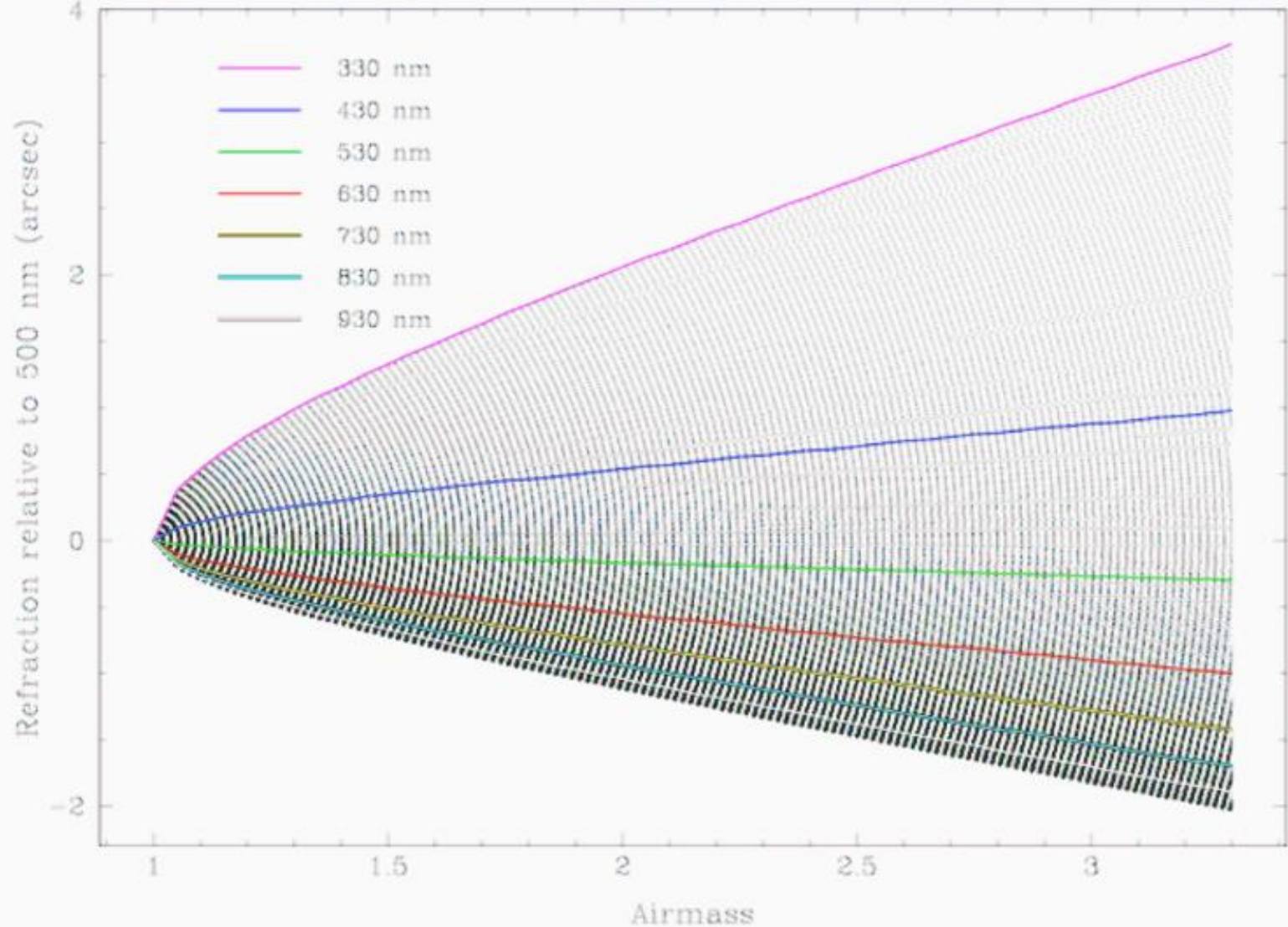
- Refraction at different atmospheric layers
- Accurate values require a full atmospheric model, taking account of P,T and n at different elevations



Atmospheric Refraction at Mauna Kea			
Zenith angle, degrees	Mauna Kea Table, arc seconds	Conventional theory, arc seconds	Lihue data, arc seconds
45°	36.70	36.80	36.81
50°	43.72	43.83	43.84
55°	52.35	52.47	52.50
60°	63.41	63.54	63.59
65°	78.35	78.48	78.56
70°	100.0	100.1	100.2
75°	134.7	134.7	135.0
80°	200.0	199.6	200.6
85°	361.8	361.6	366.5

TABLE OF ATMOSPHERIC REFRACTION AT THE MAUNA KEA OBSERVATORY, FOR $\lambda = .633$ MICRONS. THE FIRST COLUMN ARE OBSERVATIONS ANGLES RELATIVE TO THE OBSERVER'S ZENITH. THE SECOND COLUMN IS A REFRACTION TABLE AT THE MAUNA KEA OBSERVATORY. THE THIRD COLUMN WAS CALCULATED FROM THE CONVENTIONAL PARAMETERS. THE FOURTH COLUMN WAS CALCULATED FROM A LEAST SQUARES FIT TO THE LIHUE DATA FOR THE RATIO PRESSURE/TEMPERATURE DEPENDENCE ON ALTITUDE. IN KAUAI, ON AUGUST 20,2016.

Differential Atmospheric Refraction on Mauna Kea (330 nm – 1.03 μm)



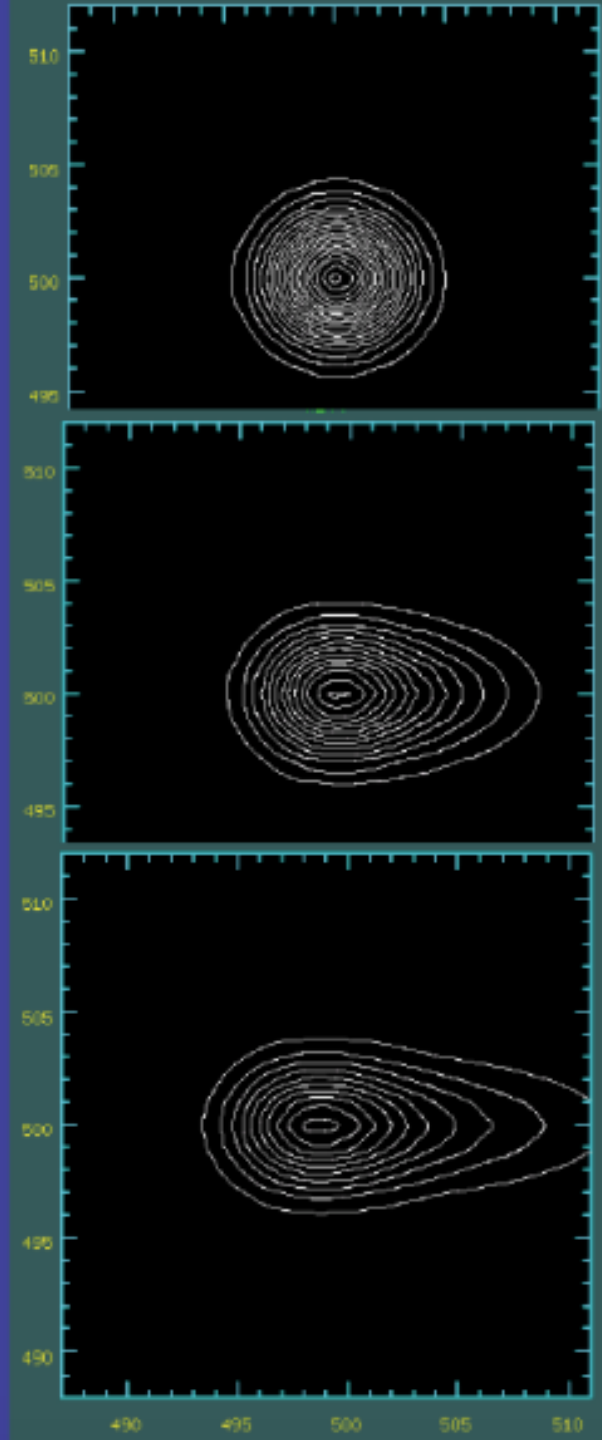
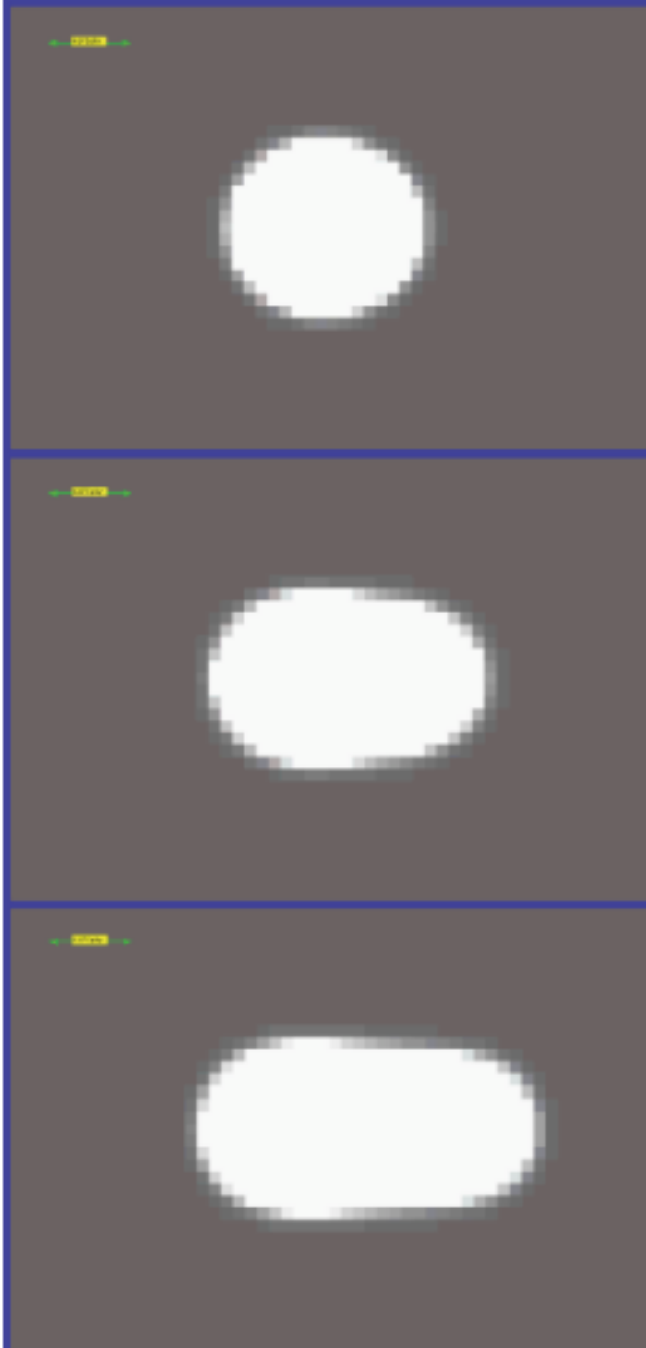
The atmospheric refractive index increases with decreasing wavelength so that blue wavelengths suffer greater refraction than red, leading to dispersion. Dispersion increases rapidly with zenith distance. The plot shows the dispersion as $\sec(Z)$ ranges from 1.1 to 3 airmass (Gemini GMOS web pages)

Differential atmospheric refraction effects are more pronounced at shorter wavelengths and under good seeing conditions.

The effect of differential atmospheric refraction (relative to 500 nm) on Mauna Kea (model) for a point source image with disk seeing of 0.3" and at three different airmasses (1.05, 1.5 and 2.0)

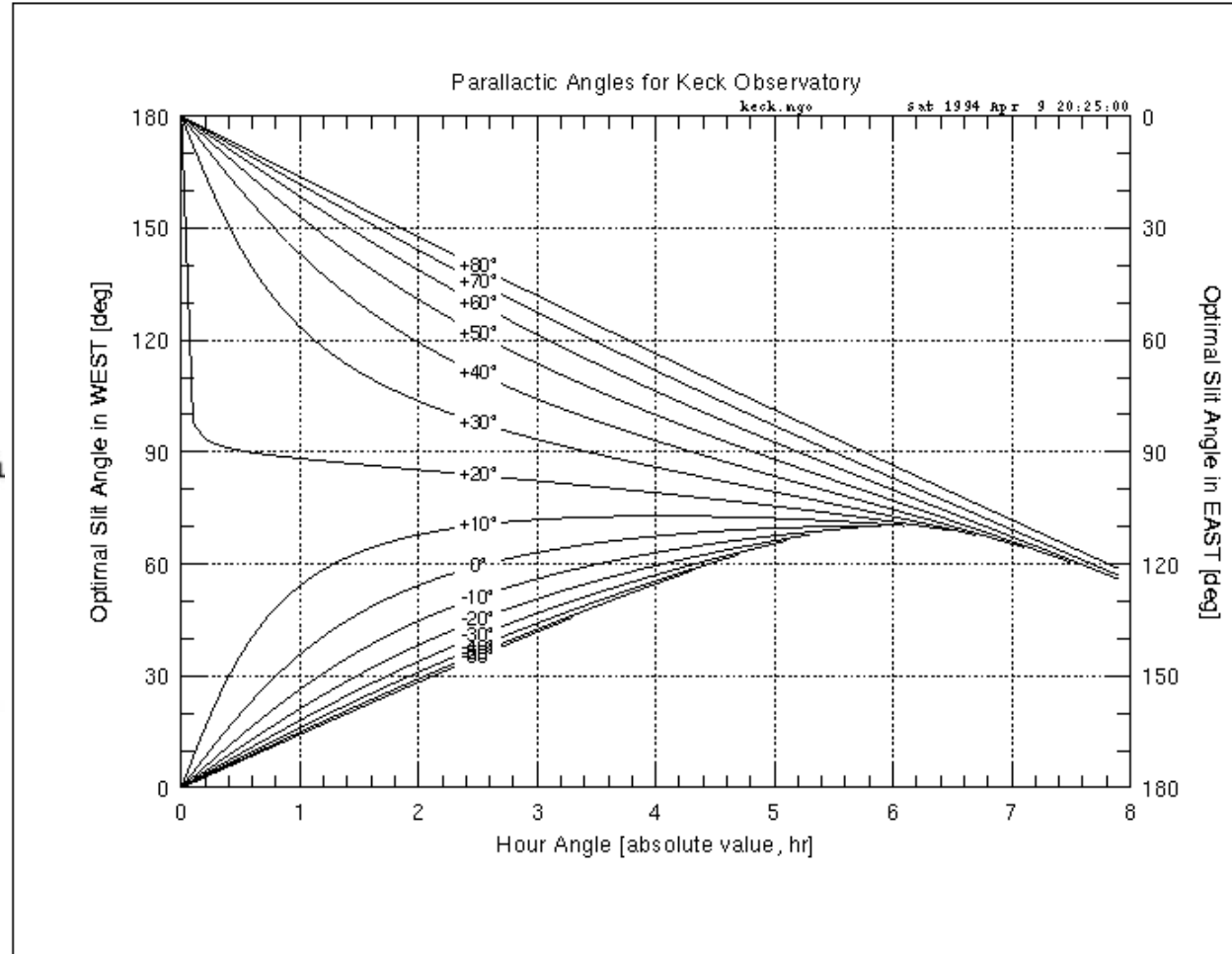
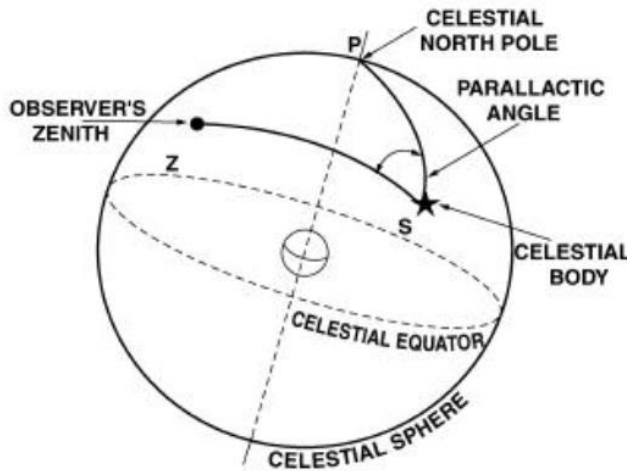
Observations in the g' filter (wavelength range 398-552 nm): the model star looks strongly elongated, particularly at airmasses 1.5 and 2

The effects are much lower in the IR, but may be important for wide-field IR instruments with AO correction



Parallactic Angle for Mauna Kea:

Latitude $19^{\circ} 45' \text{ N}$



The local vertical angle with respect to North at a particular Declination and Hour Angle

Atmospheric Dispersion Correction

- Many imagers incorporate an Atmospheric Dispersion compensator (a pair of prisms that can be rotated to compensate for dispersion optically)
- Even then, differential refraction and dispersion across the field of wide field instruments may be significant
- Improved image quality and narrow slits require more accurate refraction compensation.
- Careful attention to slit angles is needed to ensure that all wavelengths are admitted by a slit – observations may need to be made at the parallactic angle

Differential Refraction at Paranal

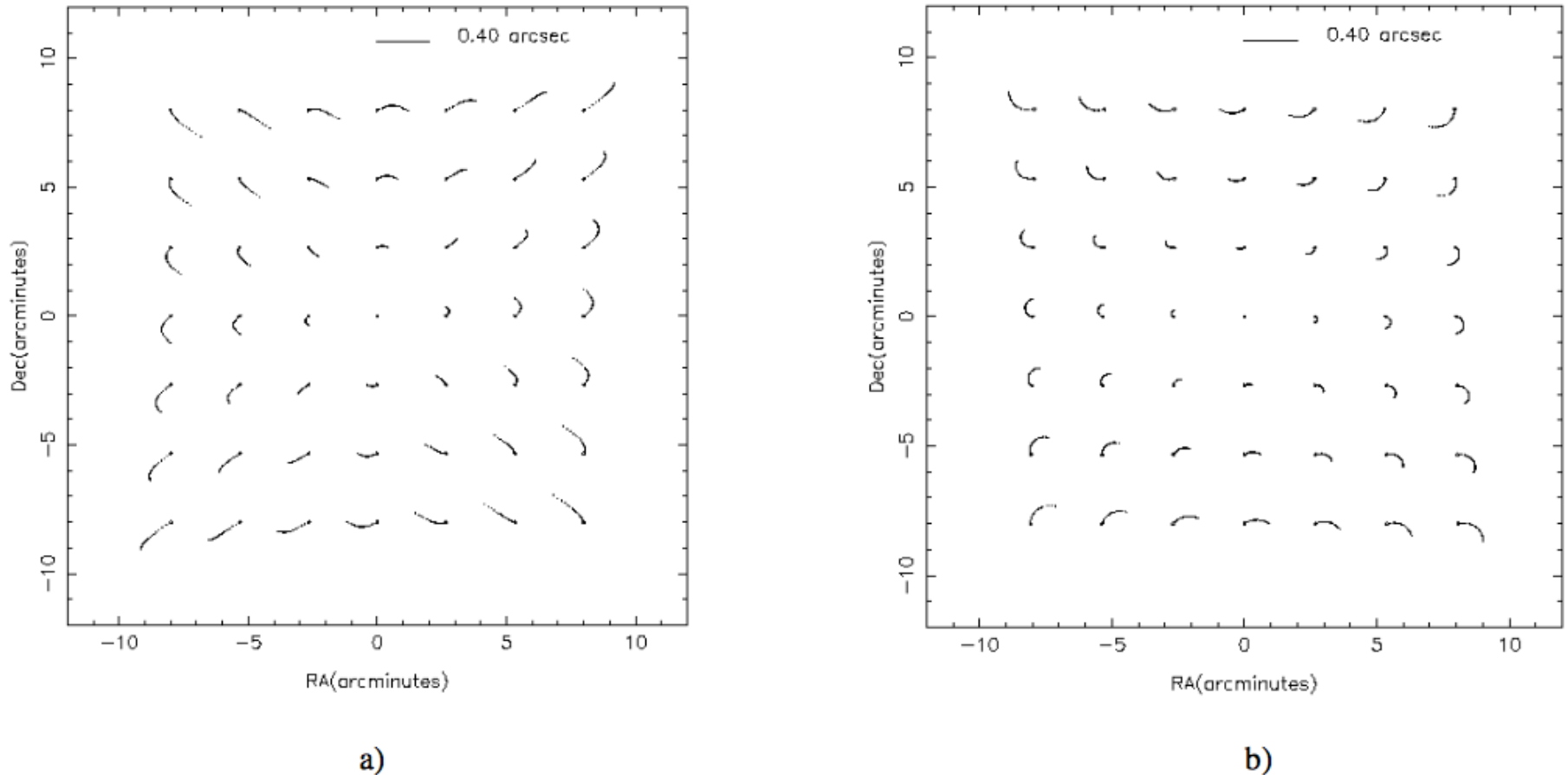


Figure 1. Field differential refraction for a 4 hour exposure starting -2 hours from meridian: a) for a northern object at a +25° declination; b) for a southern object at a -75° declination

The figure shows the differential refraction after field rotation has been compensated for a 16 x 16 arcmin field on Paranal, e.g. for the VIMOS instrument. (J-G Cuby et al)

Wide-field spectroscopy

- Observations with Multi-Object spectrographs in the visible have particular requirements that may affect observation planning
 - Differential refraction across the field changes the mean position of objects over an integration
 - Dispersion is minimised by tracking the parallactic angle
 - But the field on an alt-az telescope rotates
- Some compromise may be needed.
 - Integrations may be split over several nights so that the range of Hour Angle (and thus Parallactic angle variation) is reduced
 - For very wide-field instruments, different slit masks or fibre positions may be needed for observations at different Hour Angles
- Much more detailed treatment of these issues can be found in instrument handbooks or e.g. (Newman P.R. 2002 PASP 114 918).

Space

In space, there is no need to compensate for the atmosphere!!

Diffraction-limited optics take full advantage of unaberrated wavefronts to yield exquisite image quality and sensitivity.

This places severe constraints on the pointing and stability of spacecraft and its payload.

But

Note that the ISM is partially ionized and variations in refractive index can lead to dispersion, scattering and angular broadening at radio frequencies

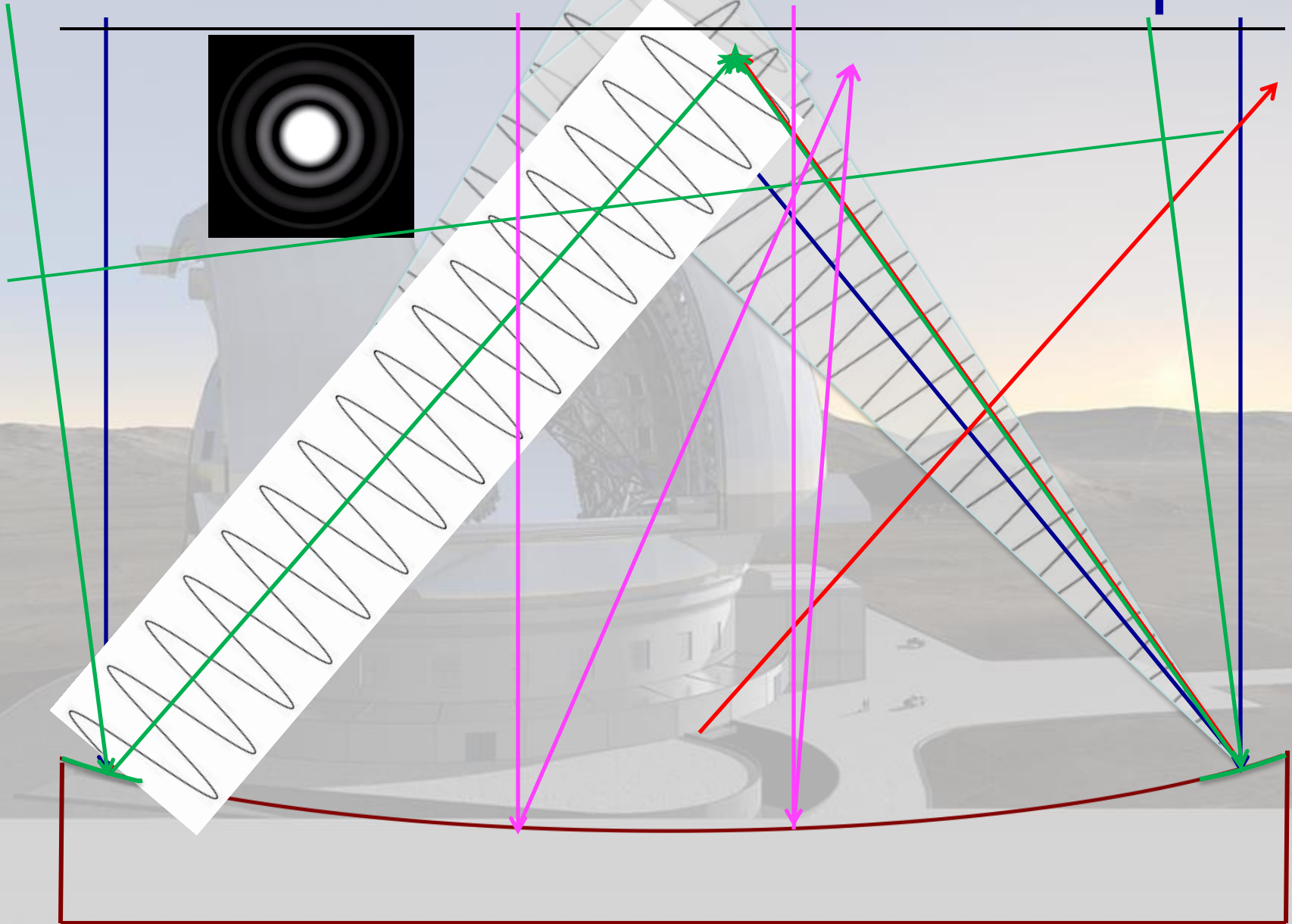
Bigger telescopes yield sharper pictures

- Results from the wave nature of light

Angular resolution = $\frac{\text{wavelength of light}}{\text{Diameter of telescope}}$

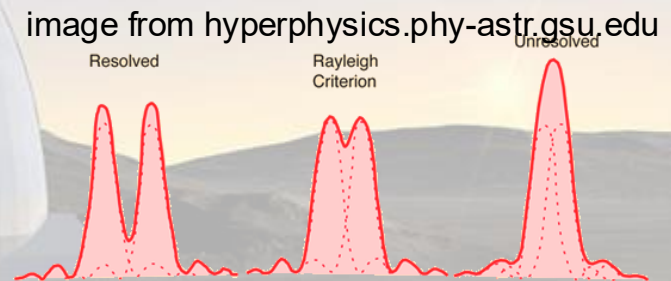
$$\theta_0 = 1.22 \frac{\lambda}{D}$$

Resolution limit of a telescope



Rayleigh resolution criterion

- Two point sources are said to be resolved when the first minimum of the diffraction pattern of one star overlaps with the peak of the other

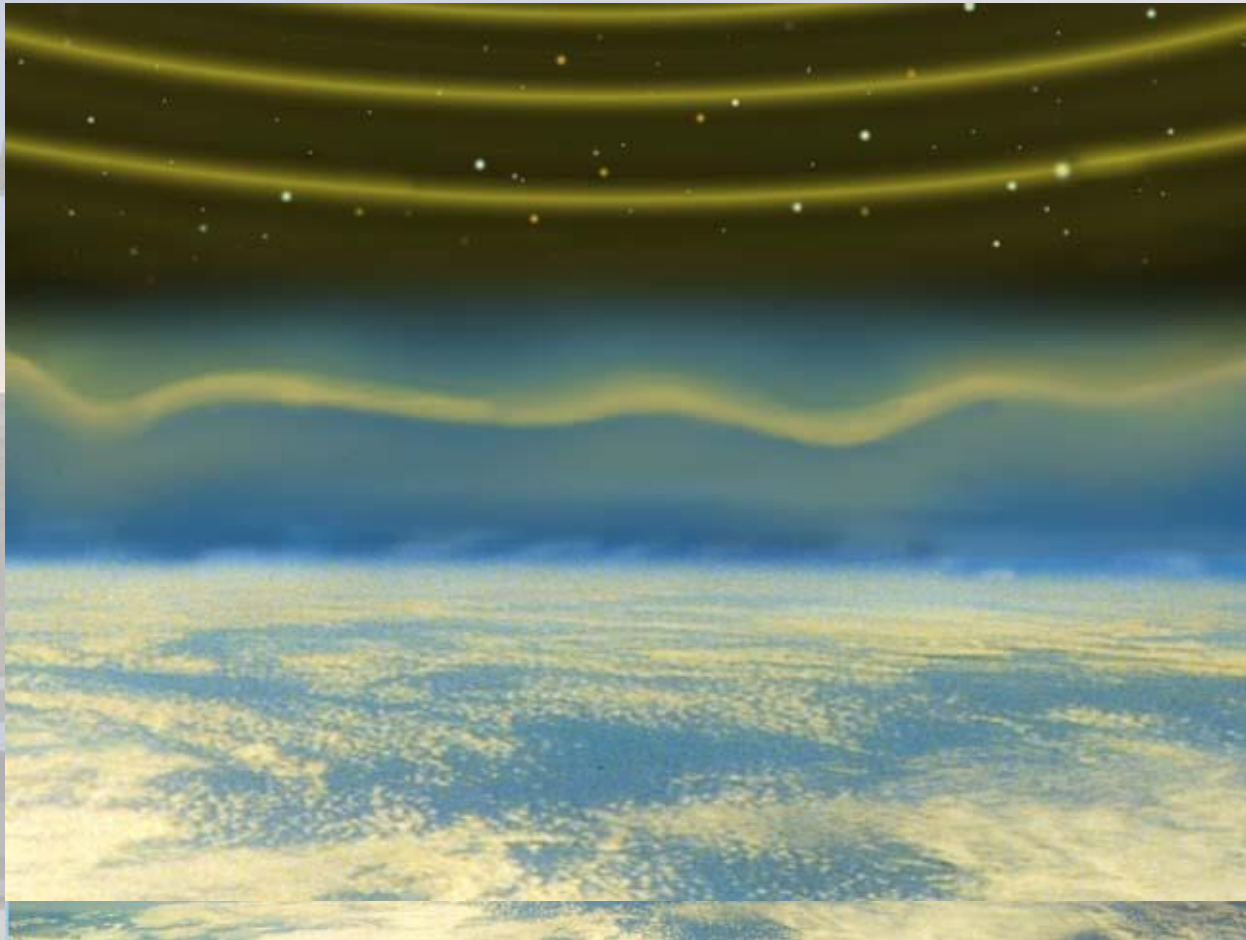


- The first minimum of the Airy pattern occurs at $\theta_{\text{lim}} = 1.22 \frac{\lambda}{D}$
- For $D = 8\text{m}$ and $\lambda = 0.5\mu\text{m}$, $\theta_{\text{lim}} = 0.015$ arcsec!

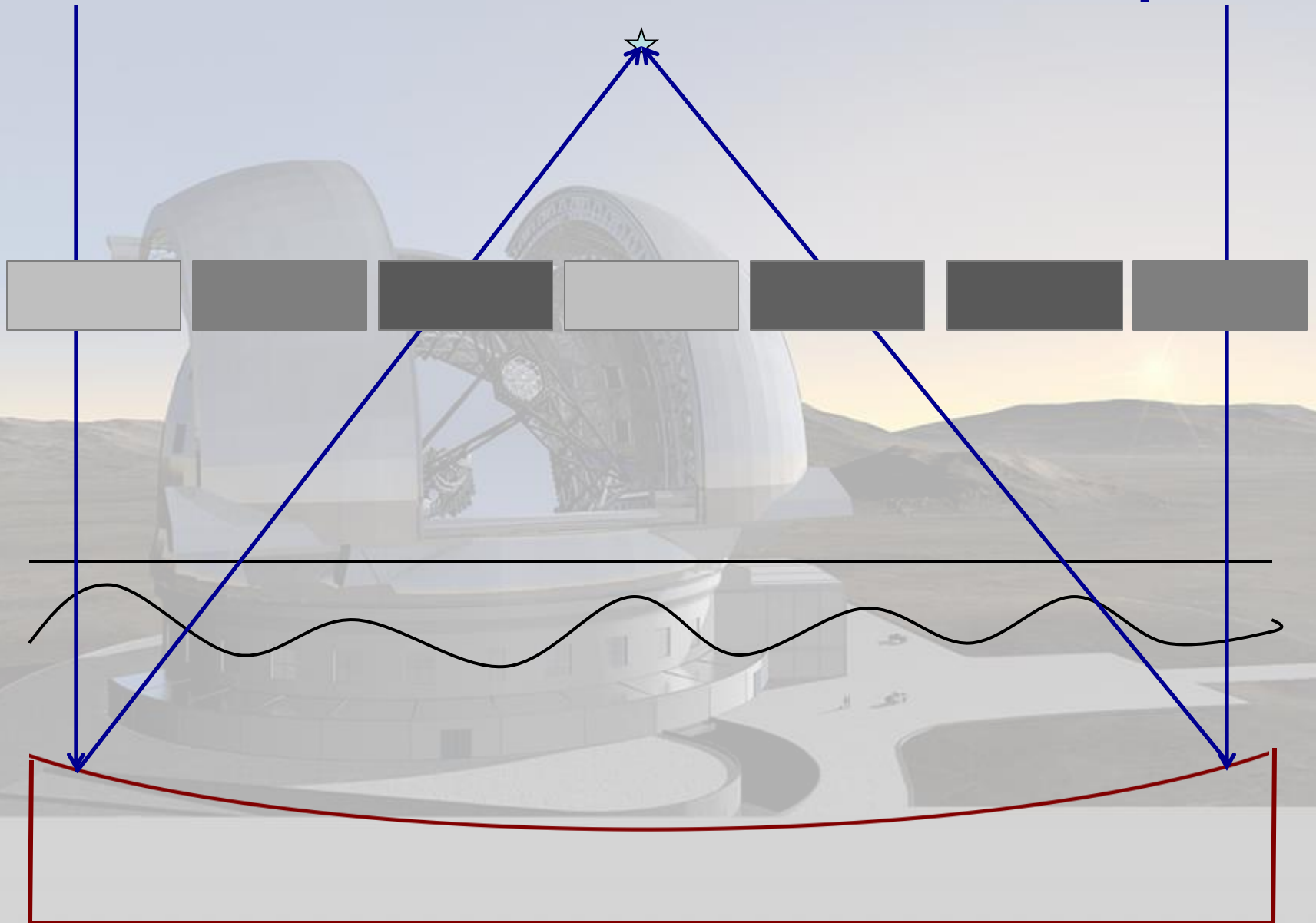
An example



Twinkle, twinkle, little star



Resolution limit of a telescope



Bigger telescopes yield sharper pictures

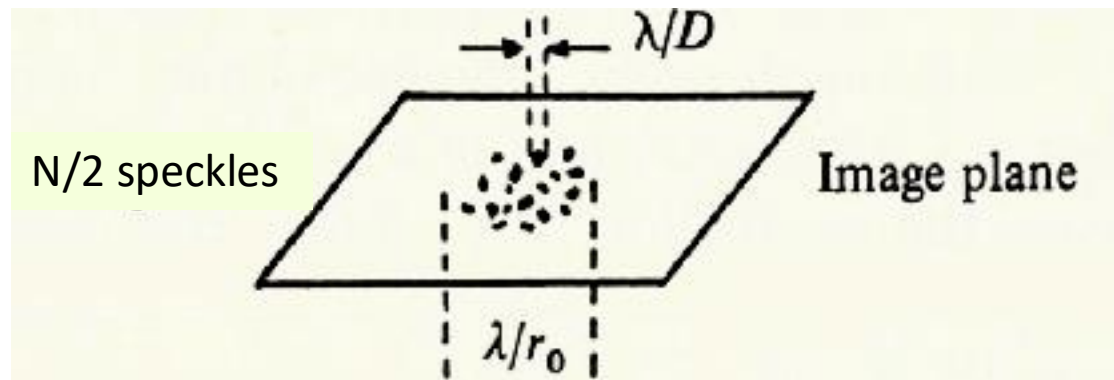
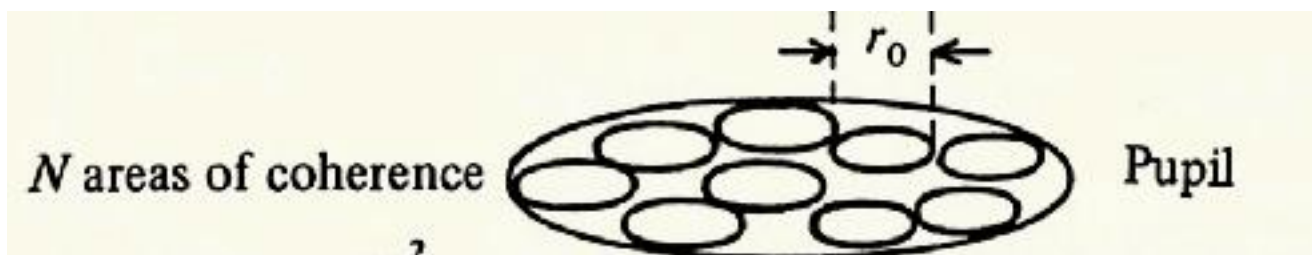
- Results from the wave nature of light

$$\text{Angular resolution} = \frac{\text{wavelength of light}}{\text{Diameter of telescope}}$$

$$\theta_0 = 1.22 \frac{\lambda}{D}$$

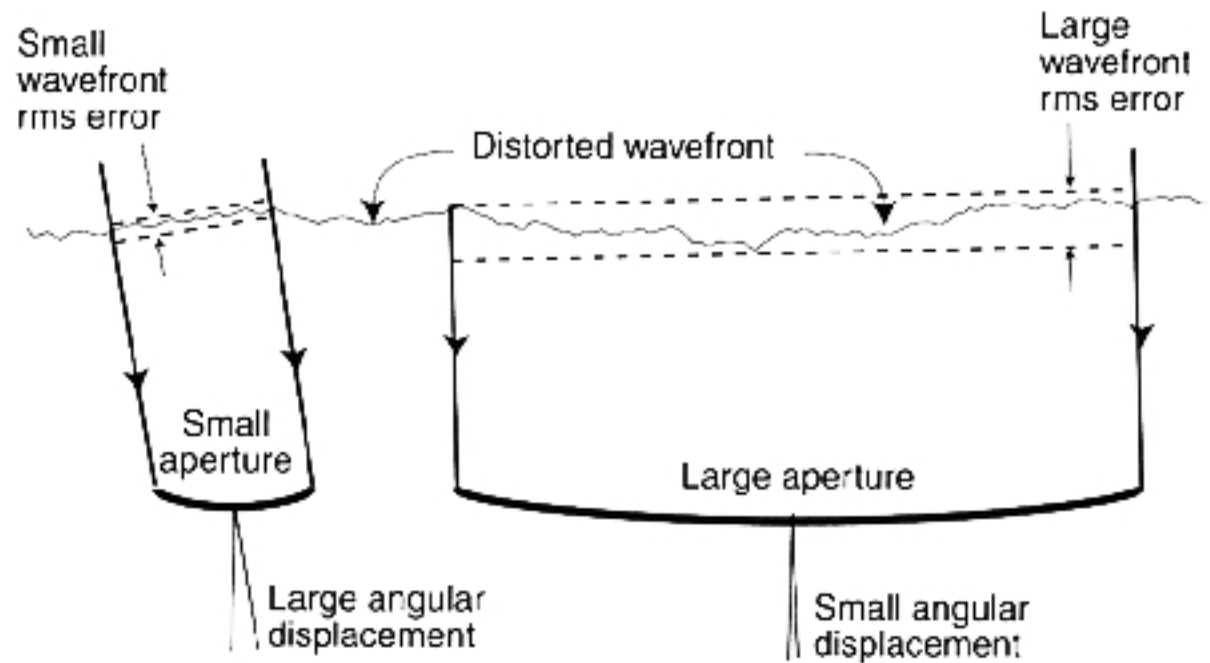
- Ground based telescopes rarely achieve the diffraction limit, as they are limited by turbulence from the earth's atmosphere.

Telescope Image



The telescope pupil contains $N = (D/r_0)^2$ cells of diameter r_0 , which produce speckles of size $\sim \lambda/D$ within the envelope given by the diffraction pattern on a scale λ/r_0 .

Image distortions



When the telescope aperture is similar to r_0 , the dominant distortion will arise from tilts in the wavefront, causing image wander.

Larger apertures encompass many r_0 and so the image will be the sum of many images blurred on a scale of λ/r_0 randomly displaced by the wavefront tilt in the subaperture.

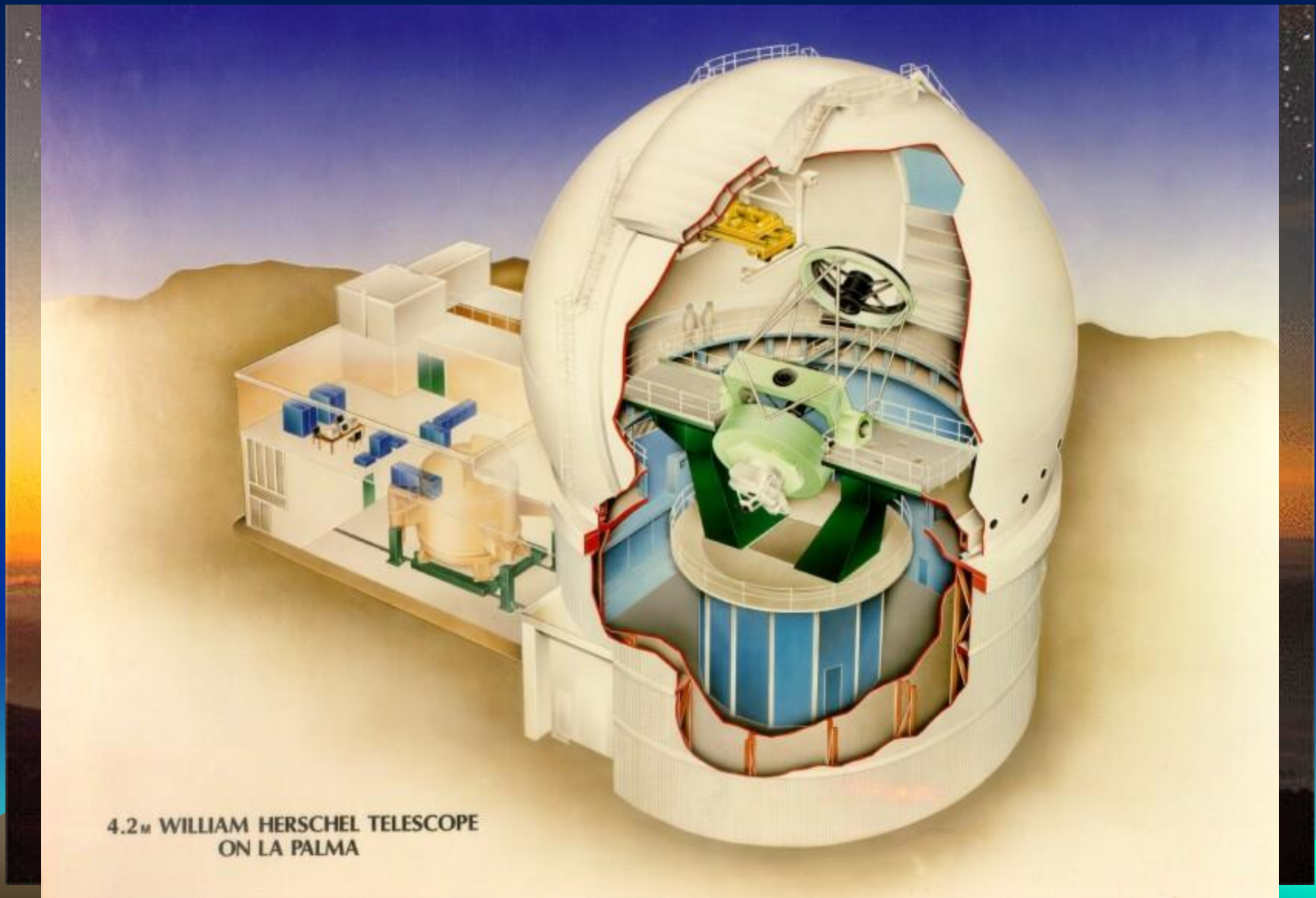
Tip-tilt correction applied to the telescope secondary can (partially) compensate for the overall wavefront tilt, and so is effective at mid-IR wavelengths on 8-m telescopes, near-IR on 4-m telescopes and amateur scale telescopes in the visible.

Similar improvements can be made by using burst mode- many short exposures that are shifted and added, discarding any poor quality images.

Or by using "Lucky Imaging", selecting only the highest quality images for coaddition. Both of these techniques impose significant overheads on the observations.

(Figure from Bely)

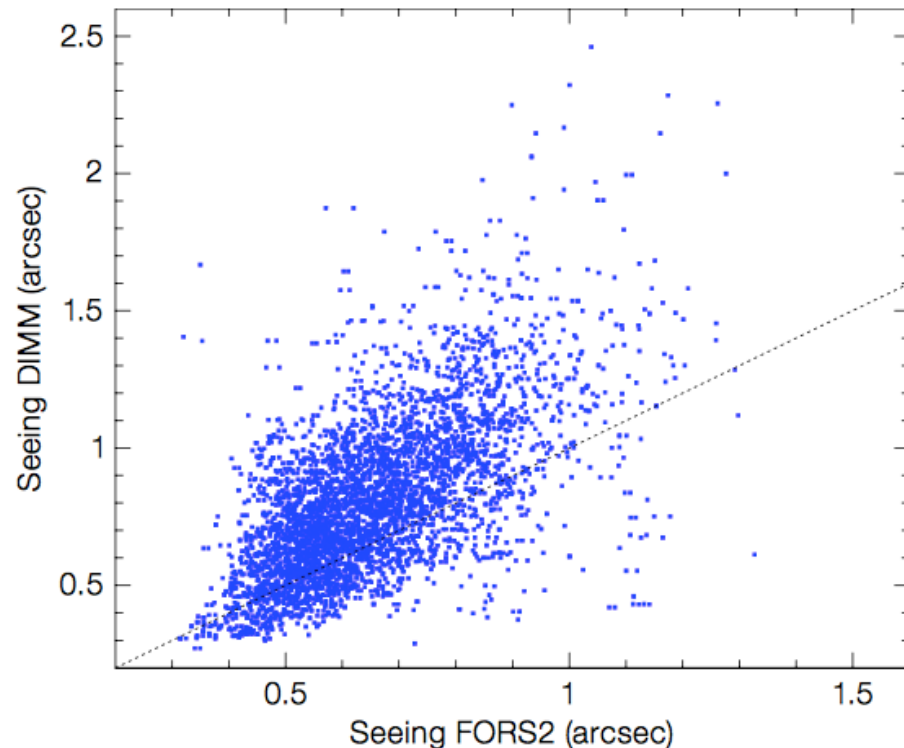
Dome seeing and ground layer



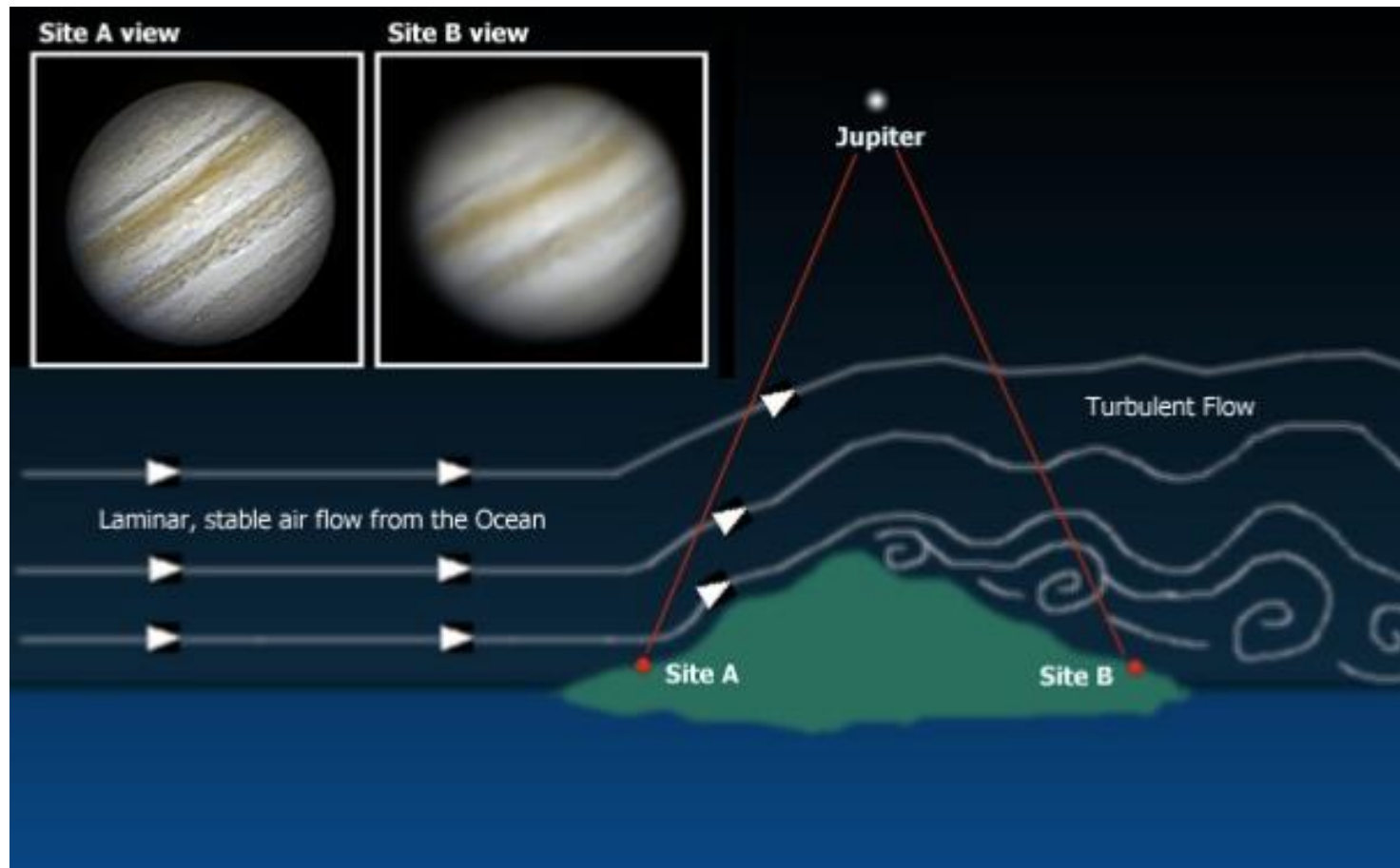
Seeing

- Turbulence along the whole path through the atmosphere contributes to the seeing
 - Jet stream can produce very fast winds, rapid changes and short coherence times
 - Local heating or topography from the mountain or the telescope dome can generate additional turbulence over the free-air profile - ground layer turbulence
 - Seeing may be seasonal or depend on wind directions etc

Many sites monitor seeing in real time using a DIMM (Differential Image Motion Monitor), but for accurate measurements the DIMM should be colocated and at the same altitude as the primary mirror

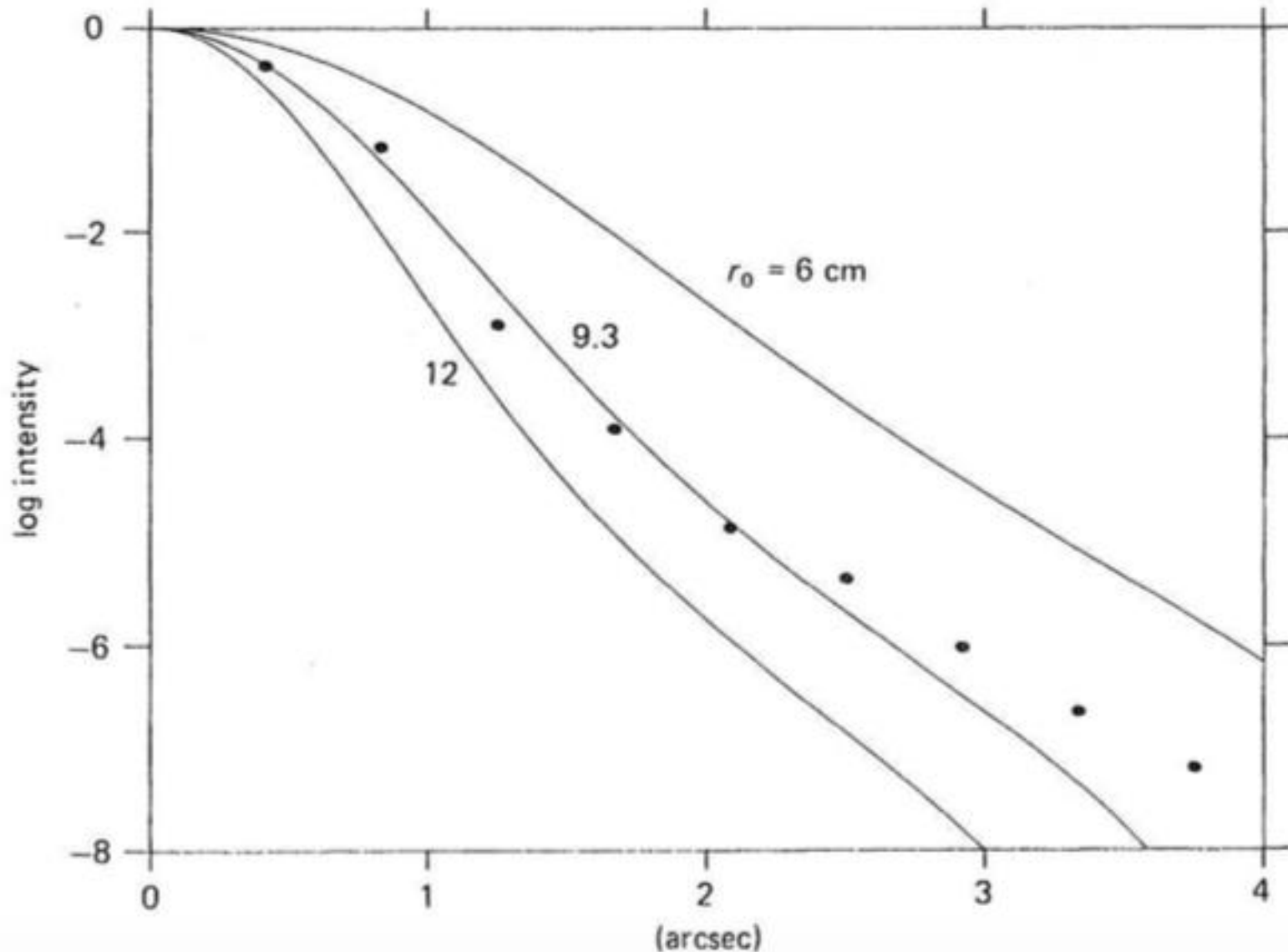


Effects of atmospheric turbulence - seeing



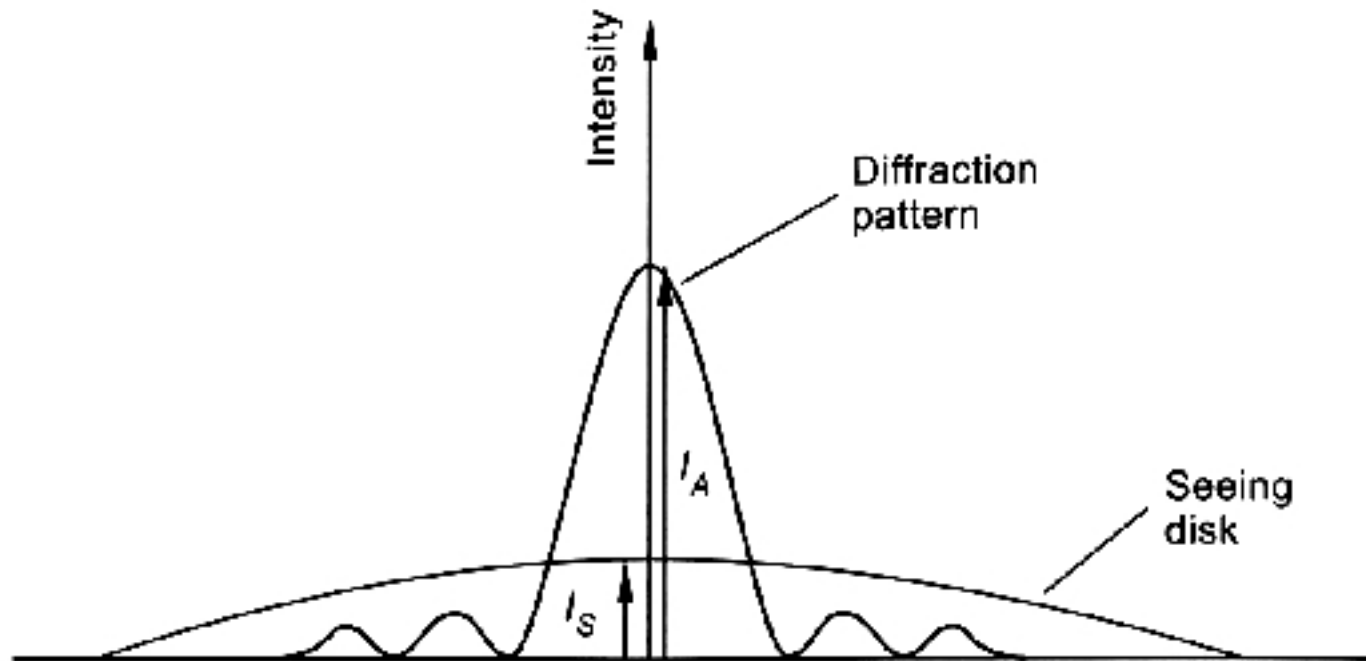
Seeing-limited images

- In long exposures, the speckle component averages out, and the resultant image is the accumulated integration of the images of size λ/r_0
- The resulting images typically have a near-gaussian core set by the transfer function of the atmosphere.
- However at large angles (>5 arcsec), scattering from mirror imperfections (scratches, splodges etc) lead to a halo which is brighter than expected for diffraction alone.
- Note that because of the wavelength dependence of seeing, stars of different colours will have slightly different profiles in wide-band images.



Theoretical long exposure image profiles for 3 different values of r_0 compared with observations (points) made in average seeing conditions at V with the CFHT on Mauna Kea. The departure beyond 3 arcsec probably represents the mirror scattering component (G Walker 1989)

Strehl Ratio



The ratio of the peak intensity of the measured image to that calculated from the diffraction pattern of the telescope optics is the Strehl Ratio